BOSE-EINSTEIN CONDENSATION OF LITHIUM - THE ROLE OF INTERACTIONS

C. A. SACKETT, C. C. BRADLEY, M. WELLING, and R. G. HULET
Physics Department and Rice Quantum Institute
Rice University
Houston, Texas 77251-1892, USA
E-mail: randy@atomcool.rice.edu

Bose-Einstein condensation of ^{7}Li has been studied in a magnetically trapped gas. Many-body quantum theory predicts that the occupation number of the condensate is limited to about 1400 atoms because of the effectively attractive interactions between ^{7}Li atoms. Using a versatile phase-contrast imaging technique, we experimentally observe the condensate number to be consistent with this limit. We discuss our measurements, the current theoretical understanding of BEC in a gas with attractive interactions, and planned experiments to observe the predicted collective collapse of the condensate.

1 Introduction

In 1995, Bose-Einstein condensation (BEC) was created in magnetically trapped atomic gases of ^{87}Rb,[1] ^{7}Li,[2] and ^{23}Na.[3] Although the condensates are very dilute gases, the interactions between atoms can still play a significant role in determining their physical properties. In the case of ^{7}Li, where the interactions are effectively attractive, it had been long believed that BEC could not occur at all in a gas.[4,5] However, it is now realized that for a trapped gas, the confining potential has a stabilizing influence, and BEC is possible for a limited number of atoms in the condensate.[6] In this report, we briefly describe the current theoretical understanding of BEC in a gas with attractive interactions, and then discuss our new measurements and their analysis. Finally, we describe some of the experiments we hope to perform in order to further investigate the dynamics of a Bose-Einstein condensate with attractive interactions.

2 Theory

Interactions between ultracold bosons may be characterized by a single parameter, the s-wave scattering length a.[7] The magnitude of a indicates the strength of the interaction, while the sign determines whether the interactions are effectively attractive ($a < 0$) or repulsive ($a > 0$). The scattering length for ^{7}Li is known to be -1.45 ± 0.04 nm.[8] Only two-body interactions need be considered for densities n such that $na^3 \ll 1$, which is the case for the experimentally

achieved densities of $n < 10^{13}$ cm^{-3}.

The effects of attractive interactions on the condensate have been studied using mean-field theory. In this approximation, the interaction part of the Hamiltonian is replaced by its mean value, resulting in an interaction energy of $U = 4\pi\hbar^2 an/m$, where m is the atomic mass.[7] Because $a < 0$, U decreases with increasing n, making the gas mechanically unstable and causing the condensate to collapse upon itself. In a system with finite volume, however, the zero-point kinetic energy of the atoms provides a stabilizing influence. For a gas at zero temperature, the net result of these effects can be determined by solving the non-linear Schroedinger equation (NLSE) for the wave function of the condensate.[7] A numerical solution to the NLSE is found to exist only when N_0 is smaller than a limiting value N_{0max}.[6] Physically, this limit can be understood as requiring that the interaction energy U be small compared to the trap level spacing $\hbar\omega$, so that the interactions act as a small perturbation to the ideal-gas solution. For ^{7}Li in our trap, the predicted limit is about 1400 atoms.

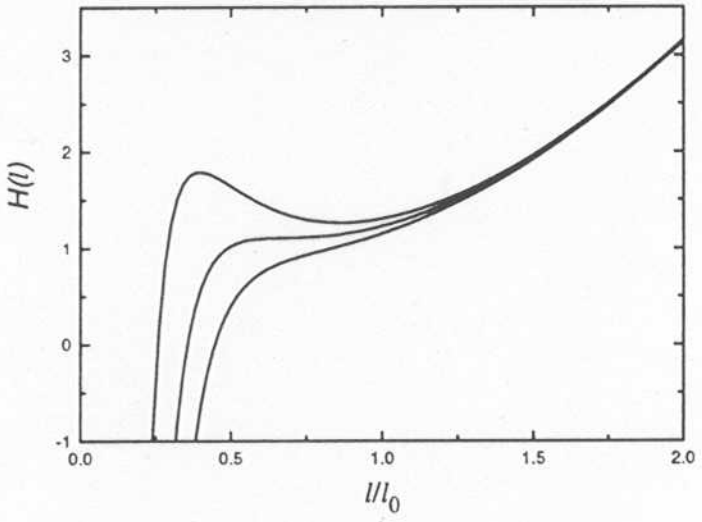

Figure 1: The condensate energy H, plotted in units of $N_0\hbar^2/ml_0^2$, where $l_0 = (\hbar/m\omega)^{1/2}$ is the length scale of the single-particle trap ground state. The upper curve corresponds to $N_0 = 0.48\,|a|/l_0$, the middle curve to $N_0 = 0.68\,|a|/l_0$, and the lower curve to $N_0 = 0.87\,|a|/l_0$. It is evident that a local minimum in H exists near $l = l_0$ if N_0 is sufficiently low, indicating that a metastable condensate can exist.

The attractive two-body interactions are expected to lead to a collective collapse of the condensate.[9,10] The presence of a tunneling barrier for collective collapse can be understood from a variational approach in which the trial wavefunction is taken to be a Gaussian.[10] Fig. 1 shows the expectation of energy H plotted versus condensate size l, when terms accounting for kinetic

energy, potential energy of confinement, and the attractive interaction energy are included. It can be seen that for sufficiently small N_0, a local minimum exists, indicating that a metastable condensate is possible. For larger N_0, however, the minimum vanishes, and the system will be unstable.

The variational model also allows exploration of the dynamics of the condensate, if l is interpreted as the coordinate of a quasiparticle moving in the potential $H(l)$. The energy levels of the quasiparticle potential then correspond to excitations of the "breathing mode" of the condensate. In particular, Stoof has calculated decay rates for the metastable state due both to thermal fluctuations and to quantum mechanical tunneling through the barrier.[10] The decay rate is found to be negligible until N_0 is within a few hundred atoms of N_{0max}, for conditions comparable to our experiments. Under our conditions, the collective collapse of the entire condensate is expected to be the dominate decay mode, as this breathing mode is the only mode found whose excitation frequency approaches zero as $N_0 \to N_{0max}$.[11]

The dynamics of the collapse itself are also interesting, but a detailed theoretical description would be difficult if the density becomes large enough that many-body interactions must be considered. However, while the density remains low, the evolution of the condensate can be described by the motion of the quasiparticle in the potential H. By calculating this trajectory and including losses due to inelastic collisions, Stoof has found that essentially all the collapsing atoms are ejected from the trap before the density rises so high that the dilute-gas approximation becomes invalid.[12] For a trapped gas at $T > 0$, only those atoms not initially in the condensate will remain after the collapse, so the gas will be in a non-equilibrium distribution. Elastic collisions rethermalize the gas, and N_0 will grow again. If the gas is actively cooled, then the condensate will continue to fill and collapse until either $T = 0$ is reached or no atoms remain. We have modeled the population dynamics of this system using the quantum Boltzmann equation, and show a typical result for $N_0(t)$ in Fig. 2. These calculations will all be elaborated upon in a future publication.[12]

3 Experiment

The apparatus used to produce BEC has been discussed in detail in previous publications.[2,13,14] The magnetic trap is an Ioffe design, constructed from six cylindrical permanent magnets. The atoms are trapped in the doubly spin polarized ground state, where they experience a nearly symmetric harmonic potential with oscillation frequencies near 150 Hz. The magnetic field at the center of the trap is directed along the z-axis, with a magnitude of 1003 G. This field configuration prevents losses due to nonadiabatic spin-flip transitions

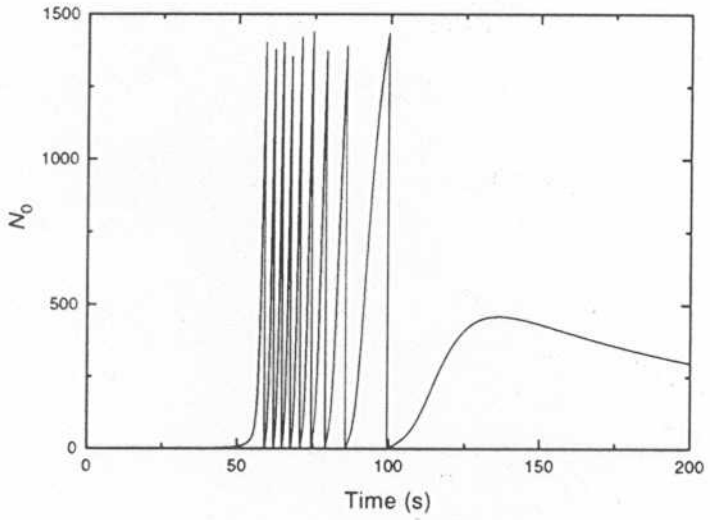

Figure 2: Evolution of the number of condensate atoms during evaporative cooling. At early times, corresponding to high temperatures, the number of condensate atoms is negligible, but as the gas is cooled to the critical point, N_0 begins to rise. When N_0 approaches the stability limit N_{0max}, the rates for thermal and quantum mechanical fluctuations increase, until eventually the condensate collapses. It is expected that the entire condensate collapses at once, effectively reducing N_0 to zero. Elastic collisions then repopulate the condensate, and the cycle continues until too few atoms remain to cause a collapse. The remaining atoms are then gradually lost through inelastic collisions.

which can occur near a field zero. The trap is loaded from a laser-slowed atomic beam, and the dissipation needed to capture the atoms is provided by six laser beams tuned near the $2S_{1/2}$ (F = 2, m_F = 2) $\leftrightarrow$ $2P_{3/2}$ (F = 3, m_F = 3) cycling transition. The number of trapped atoms N reaches a maximum of approximately 2×10^8, after a few seconds of loading. These atoms are pre-cooled to about 200 μK by Doppler laser cooling, and have a peak density of roughly 1×10^{11} cm^3.

After switching off the laser beams, the atoms are further cooled by forced evaporative cooling. The hottest atoms are driven to an untrapped ground state by a microwave field tuned just above the (F = 2, m_F = 2) $\leftrightarrow$ (F = 1, m_F = 1) Zeeman transition frequency of approximately 3450 MHz. As the atoms cool, the microwave frequency is reduced. The frequency vs. time trajectory that maximizes the phase-space density of the trapped atoms is calculated ahead of time,[15] and depends on the elastic collision rate and the trap loss rate. The elastic collision rate $n\sigma v$ is roughly 1 s^{-1}, with cross-section $\sigma = 8\pi a^2 \approx 5 \times 10^{-13}$ cm^2. The collision rate is approximately constant during evaporative cooling. The loss rate due to collisions with hot background gas atoms is 1.6×10^{-3} s^{-1}, and inelastic dipolar-relaxation collisions occur with

a rate constant of 10^{-14} cm^3/s.[16] Quantum degeneracy is typically reached after roughly 200 seconds, with $N \approx 10^5$ atoms at $T \approx 300$ nK, although fluctuations in the loading conditions produce some variation in the results of evaporative cooling. Lower temperatures are reached by extending the cooling time.

After evaporative cooling, the rf field is removed, and the atoms are allowed to equilibrate for a few seconds. The spatial distribution of atoms is then imaged *in situ* using an optical probe. The single-particle harmonic oscillator ground state of our trap has a Gaussian density distribution with a $1/e$-radius of 3 μm. The resolution of the imaging system must therefore be sufficient to detect such a small object. In our original experiment,[2] the imaging resolution was not sufficient, but the presence of the condensate was deduced from distortions observed in images of quantum degenerate clouds. We have since developed a comprehensive model of these distortions, which is explained in detail in ref.[17]. In that work, we find that the presence of a condensate should cause such distortions, given the imaging system that was used.

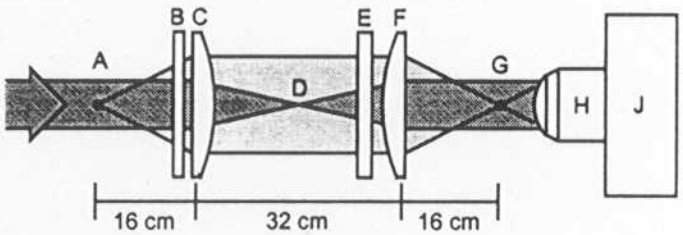

Figure 3: A schematic of the imaging system used for *in situ* phase-contrast polarization imaging. A linearly polarized laser beam is directed through the cloud of trapped atoms located at A. The probe beam and scattered light field pass out of a vacuum viewport B, and are relayed to the primary image plane G by an identical pair of 3-cm-diameter, 16-cm-focal-length doublet lenses C and F. The light is then re-imaged and magnified onto a camera J by a microscope objective H. The measured magnification is 19, and the camera pixels are 19 μm square. A linear polarizer E can be used to cause the scattered light and probe fields to interfere, producing an image sensitive to the refractive index of the cloud. The system is focussed by adjusting the position of lens F, which is mounted on a translator. Reprinted from Ref.[13] by permission.

We have subsequently improved our imaging, and now use a system shown schematically in Fig. 3. With the polarizer E removed, it can be used to measure the density distribution by absorption imaging, in which the absorptive shadow of the atoms is imaged onto the camera. However, the atom cloud causes both an attenuation and a phase shift of the probe laser beam. Near resonance, the phase shift can be large, and any imaging system with finite resolution will be sensitive to this phase to some extent. This sensitivity can

cause significant image distortions, which are readily detected through their dependence on the probe detuning Δ. In order to eliminate such distortions, it is necessary to reduce the index of refraction by using large Δ. However, since the absorption coefficient decreases as Δ^{-2}, while the phase shift decreases as only Δ^{-1}, eliminating the distortions can leave the absorption signal too small to be detected.

This problem can be solved by using phase-contrast imaging, a common technique in microscopy. We have developed a sensitive method for phase-contrast imaging, in which the signal depends linearly on the dispersive phase shift, by exploiting the birefringence of the atoms in a strong magnetic field.[13] By passing the probe light through a polarizer (E in Fig. 3), the scattered light and probe light can be made to interfere, thereby producing a signal proportional to their relative phase.

The probe beam is pulsed on for a duration of 10 μs, at an intensity of 250 mW/cm^2 and with Δ in the range $20\Gamma < |\Delta| < 40\Gamma$, where $\Gamma = 5.9$ MHz is the natural linewidth of the transition. Only one image can be obtained under these conditions, because each atom scatters a few photons while being probed, heating the gas to several μK. The detected signal intensity is proportional to the column density of the trapped atoms.

Fig. 4 shows radial signal profiles, which are obtained from the images by angle-averaging the data around the ellipse defined by the trapping potential. The various curves are the results of our analysis, which will be described in the following section.

4 Image Analysis

We assume that the gas is in thermal equilibrium, and fit T and N_0 to the data. Any two of N, T, or N_0 completely determine the density of the gas through the Bose-Einstein distribution function. Given T and N_0, the density is calculated using a semi-classical ideal-gas approximation for the non-condensed atoms,[18] and a Gaussian function for the condensate. The semi-classical distribution was compared to an exact calculation, and found to be accurate, except for a temperature shift as noted in ref.[19]. The results of the fits are shown by the solid lines in Fig. 4.

For temperatures sufficiently greater than the critical temperature, the gas can be described by the Boltzmann distribution, which predicts a Gaussian density profile. The long-dashed lines in Fig. 4 are Gaussian functions fit to the tails of the distributions, which approximate the data only in Fig. 4(a), where the fit to the Bose-Einstein distribution indicates a near-degenerate condition, with $N_0 \approx 1$. Fig. 4(b) shows three distributions for which $N_0 \gg 1$. For

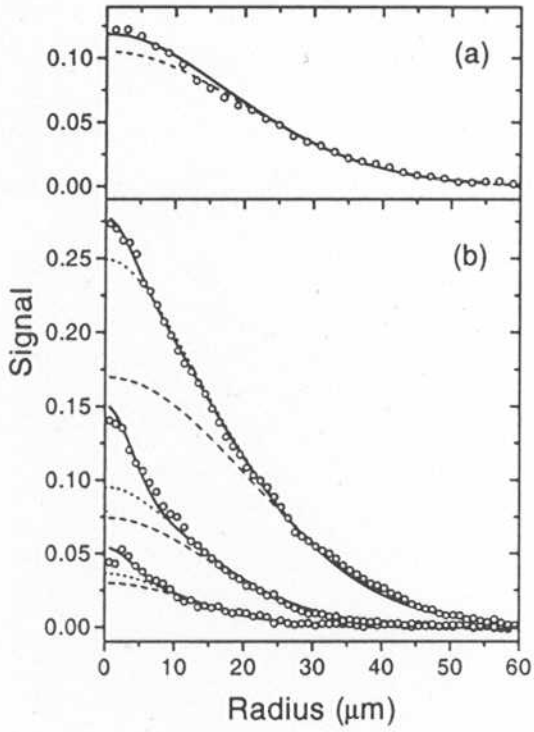

Figure 4: Spatial image profiles of trapped ultracold ^{7}Li gas. The vertical axis gives the magnitude of the phase-contrast signal intensity relative to the probe intensity, which is proportional to the column density of the gas. The data points are taken from observed images. The solid curves are calculated by fitting Bose-Einstein distributions to the data, the short-dashed curves are the same distributions with the condensate atoms removed, and the long-dashed curves are classical (Gaussian) distributions fit to the tails of the data. The calculated signals are convolved with a Gaussian function to account for the limited resolution of the imaging system, assuming an effective resolution of 4 μm. For the data in (a), the probe detuning was +191 MHz, and the fitted distribution has 9.0×10^4 atoms at a temperature of 309 nK. The number of condensate atoms is $\sim$1, indicating that the gas is just approaching degeneracy. In (b) a sequence of profiles that exhibit condensate peaks are shown. From the strongest to weakest signals, the total number of atoms and fitted temperatures are: 1.01×10^5 atoms at 304 nK; 2.6×10^4 atoms at 193 nK; and 6.6×10^3 atoms at 122 nK. The corresponding numbers of condensate atoms are 500, 810, and 270, respectively. The probe laser detuning for these data was -130 MHz. Reprinted from Ref. [13] by permission.

these distributions, the density is distinctly non-Gaussian, due to an enhanced central peak. Comparison between Fig. 4(a) and the upper curve in Fig. 4(b) is striking, as these distributions correspond to nearly the same temperature, but differ by only about 10% in number. From this comparison, it is clear that the gas has reached the degenerate regime, where Boltzmann statistics are inadequate.

Using the fitting procedure described above, we have found degenerate conditions for T between 120 and 330 nK, and for N between 6,800 and 135,000 atoms. In all cases, N_0 is found to be less than 1300 atoms. The uncertainty in focal position of the imaging lens is the dominant source of error in our determination of N_0 and leads to an uncertainty of about a factor of two.[17]

In the analysis so far we have assumed that the gas is ideal, but interactions are expected to alter the size and shape of the density distribution. Mean-field theory predicts that interactions will reduce the $1/e$-radius of the condensate from 3 μm for low occupation number to $\sim$2 μm as the maximum N_0 is approached.[20,10] If the smaller condensate radius is assumed in the analysis, the maximum observed value for N_0 decreases, becoming $\sim$1050. The size of the condensate is not expected to change appreciably for $N_0 < 1000$. Effects of the interactions on the distribution of the non-condensed atoms are not expected to be significant, because at the critical density the mean interaction energy of $\sim$1 nK is much smaller than T.

5 Conclusions and Future Experiments

The measurements described above have demonstrated that BEC can occur in a gas with $a < 0$. The results of our analysis indicate a number of condensate atoms which is consistent with the limit predicted by mean-field theory.

An exciting prospect for the future is to experimentally study the collapse itself. The collective collapse of the condensate is predicted to occur by either macroscopic quantum tunneling through the barrier shown in Fig. 1, or by thermal excitation of the entire condensate over the same barrier. The collapse/fill model described in §2 predicts that the values of N_0 should fluctuate between zero and the limiting value during evaporative cooling. We have observed fluctuations in N_0, but it is not clear whether they are intrinsic or whether they are caused by variations in trap loading and evaporative cooling. If these variations can be controlled and N_0 measured precisely, then measurement of the fluctuations should provide detailed information on the dynamics of the collapse and growth of the condensate. Thus a negative scattering length condensate may be one of the few areas in physics for which macroscopic quantum tunneling can be explored experimentally. We believe that, through experiments such as these, studies of condensates with $a < 0$ will provide important insights into many-body quantum theory.

Acknowledgments

We are grateful to H. Stoof for many stimulating discussions. This work is supported by the NSF, the Welch Foundation, the Texas Advanced Technology Program, and NASA. M.W. acknowledges support from the Deutsche Forschungsgemeinschaft.

References

1. M. H. Anderson, J. R. Ensher, M. R. Matthews, C. E. Wieman, and E. A. Cornell. Observation of Bose-Einstein condensation in a dilute atomic vapor. *Science*, 269:198, 1995.
2. C. C. Bradley, C. A. Sackett, J. J. Tollett, and R. G. Hulet. Evidence of Bose-Einstein condensation in an atomic gas with attractive interactions. *Phys. Rev. Lett.*, 75:1687, 1995.
3. K. B. Davis, M.-O. Mewes, M. R. Andrews, N. J. van Druten, D. S. Durfee, D. M. Kurn, and W. Ketterle. Bose-Einstein condensation in a gas of sodium atoms. *Phys. Rev. Lett.*, 75:3969, 1995.
4. L. D. Landau and E. M. Lifshitz. *Statistical Physics.* Pergamon, London, 1st edition, 1958.
5. H. T. C. Stoof. Atomic Bose gas with a negative scattering length. *Phys. Rev. A*, 49:3824, 1994.
6. P. A. Ruprecht, M. J. Holland, K. Burnett, and M. Edwards. Time-dependent solution of the nonlinear Schrodinger equation for Bose-condensed trapped neutral atoms. *Phys. Rev. A*, 51:4704, 1995.
7. K. Huang. *Statistical Mechanics.* John Wiley & Sons, New York, 2 edition, 1987.
8. E. R. I. Abraham, W. I. McAlexander, C. A. Sackett, and R. G. Hulet. Spectroscopic determination of the *s*-wave scattering length of lithium. *Phys. Rev. Lett.*, 74:1315, 1995.
9. Y. Kagan, G. V. Shlyapnikov, and J. T. M. Walraven. Bose-Einstein condensation in trapped atomic gases. *Phys. Rev. Lett.*, 76:2670, 1996.
10. H. T. C. Stoof. Atomic Bose gas with a negative scattering length. *J. Stat. Phys.*, 87:1353, 1997.
11. K.G. Singh and D.S. Rokhsar. Collective excitations of a confined Bose gas. *Phys. Rev. Lett.*, 77:1667, 1996.
12. C. A. Sackett, H. T. C. Stoof, and R. G. Hulet, to be published.
13. C. C. Bradley, C. A. Sackett, and R. G. Hulet. Bose-Einstein condensation of lithium: Observation of limited condensate number. *Phys. Rev. Lett.*, 78:985, 1997.

14. J. J. Tollett, C. C. Bradley, C. A. Sackett, and R. G. Hulet. Permanent magnet trap for cold atoms. *Phys. Rev. A*, 51:R22, 1995.
15. C. A. Sackett, C. C. Bradley, and R. G. Hulet. Optimization of evaporative cooling. *Phys. Rev. A*, 55:3797, 1997.
16. A. J. Moerdijk and B. J. Verhaar. Collisional two- and three-body decay rates of dilute quantum gases at ultralow temperatures. *Phys. Rev. A*, 53:R19, 1996.
17. C. C. Bradley, C. A. Sackett, and R. G. Hulet. Analysis of in situ images of Bose-Einstein condensates of lithium. *Phys. Rev. A*, 55:3951, 1997.
18. V. Bagnato, D. E. Pritchard, and D. Kleppner. Bose-Einstein condensation in an external potential. *Phys. Rev. A*, 35:4354, 1987.
19. W. Ketterle and N. J. van Druten. Bose-Einstein condensation of a finite number of particles trapped in one or three dimensions. *Phys. Rev. A*, 54:656, 1996.
20. F. Dalfovo and S. Stringari. Bosons in anisotropic traps: Ground state and vortices. *Phys. Rev. A*, 53:2477, 1996.